

PAPER

## Focused-ion-beam assisted technique for achieving high pressure by uniaxial-pressure devices

To cite this article: Di Liu *et al* 2023 *Chinese Phys. B* **32** 047401

View the [article online](#) for updates and enhancements.

### You may also like

- [Nonlinear uniaxial pressure dependence of the resistivity in  \$\text{Sr}\_{1-x}\text{Ba}\_x\text{Fe}\_{1-y}\text{Ni}\_y\text{As}\_2\$](#)   
Hui-Can Mao, , Dong-Liang Gong et al.
- [Control of the electronic states of  \$\text{Ca}\_2\text{RuO}\_4\$  by uniaxial pressure](#)  
Ryo Ishikawa, Haruka Taniguchi, Swee Kuan Goh et al.
- [In-Plane Anisotropic Response to Uniaxial Pressure in the Hidden Order State of  \$\text{URu}\_2\text{Si}\_2\$](#)   
Xingyu Wang, , Dongliang Gong et al.

# Focused-ion-beam assisted technique for achieving high pressure by uniaxial-pressure devices

Di Liu(刘迪)<sup>1,2</sup>, Xingyu Wang(王兴玉)<sup>1,2</sup>, Zezhong Li(李泽众)<sup>1,2</sup>,  
Xiaoyan Ma(马肖燕)<sup>1,2</sup>, and Shiliang Li(李世亮)<sup>1,2,3,†</sup>

<sup>1</sup>Beijing National Laboratory for Condensed Matter Physics, Institute of Physics, Chinese Academy of Sciences, Beijing 100190, China

<sup>2</sup>School of Physical Sciences, University of Chinese Academy of Sciences, Beijing 100190, China

<sup>3</sup>Songshan Lake Materials Laboratory, Dongguan 523808, China

(Received 4 November 2022; revised manuscript received 9 December 2022; accepted manuscript online 16 December 2022)

Uniaxial pressure or strain can introduce a symmetry-breaking distortion on the lattice and may alter the ground states of a material. Compared to hydrostatic pressure, a unique feature of the uniaxial-pressure measurements is that a tensile force can be applied and thus a “negative” pressure can be achieved. In doing so, both ends of the sample are usually glued on the frame of the uniaxial-pressure device. The maximum force that can be applied onto the sample is sometimes limited by the shear strength of the glue, the quality of the interface between the sample and the glue, etc. Here we use focused ion beam to reduce the width of the middle part of the sample, which can significantly increase the effective pressure applied on the sample. By applying this technique to a home-made piezobender-based uniaxial-pressure device, we can easily increase the effective pressure by one or two orders of magnitude as shown by the change of the superconducting transition temperature of an iron-based superconductor. Our method thus provides a possible way to increase the upper limit of the pressure for the uniaxial-pressure devices.

**Keywords:** uniaxial pressure, iron-based superconductors, focused-ion-beam

**PACS:** 74.62.Fj

**DOI:** 10.1088/1674-1056/acac1a

## 1. Introduction

The uniaxial-pressure or uniaxial-strain technique has been rapidly developed due to its unique role played in studying strongly correlated materials in condensed matter physics. The change of strain along a particular lattice axis can be coupled to a symmetry-breaking order parameter, such as the nematic order, and thus act as a conjugate field to it.<sup>[1]</sup> This idea has been widely used in studying nematic fluctuations in iron-based superconductors and some other systems to obtain nematic susceptibility,<sup>[2-9]</sup> although one should be cautious not to attribute any uniaxial dependence of physical properties to nematicity.<sup>[10-12]</sup> In these cases, the required uniaxial pressure or strain is small since the susceptibility is only well defined when the conjugated field is close to zero,<sup>[13]</sup> just as measuring magnetic susceptibility under a magnetic field. When the pressure or strain is large, many properties of a system can be significantly tuned and even the ground states can be changed.<sup>[14-18]</sup> This makes it a power tool in studying strongly correlated electron systems since there are usually various competing orders, which make the system more sensitive to the change of lattice. In this sense, the uniaxial pressure technique is similar to the hydrostatic pressure technique except that the latter is not symmetry-breaking. However, a unique feature of the uniaxial pressure is that a negative pressure or positive strain can be achieved, which provides us more

opportunities in tuning the ground states.

One of the designs for the uniaxial-pressure devices is based on piezoelectric materials, which can provide *in-situ* continuous control of the uniaxial pressure or strain at low temperatures and high magnetic fields. These kinds of devices include a commercial available one based on three piezoelectric stacks,<sup>[19]</sup> which can provide large strain tuning. The two ends of a thin-plate sample need to be attached on the supporting plates by epoxy. The force that can be applied to the sample is thus limited by the interfaces between the sample and the epoxy, since the maximum shear pressure that the epoxy can be endured is relatively small. Moreover, since the force is mostly transferred by such interfaces, asymmetry and inhomogeneity of the strain may happen. We have also developed a similar uniaxial pressure device based on piezobender,<sup>[5,6,20]</sup> which provides an easier method to apply uniaxial pressure but the maximum force is small due to the limit of the piezobender.

In this work, we use the focused-ion-beam (FIB) technique to reduce the cross section of the sample on the piezobender-based uniaxial-pressure device, which effectively increases the uniaxial pressure for the same force. By measuring the uniaxial pressure dependence of the superconducting transition temperature  $T_c$  of an iron-based superconductor  $\text{BaFe}_{1.83}\text{Ni}_{0.17}\text{As}_2$ , we show that the maximum pressure can be increased dramatically, changing from tens of MPa to

<sup>†</sup>Corresponding author. E-mail: slli@iphy.ac.cn

about 2 GPa. This method not only can increase the maximum pressure applied on the sample but also has a few advantages that may help us study the uniaxial pressure dependence of the physical properties of materials.

## 2. Experiments

Single crystals of  $\text{BaFe}_{1.83}\text{Ni}_{0.17}\text{As}_2$  ( $T_c \approx 12$  K) were grown by the self-flux method reported previously.<sup>[21]</sup> The as-grown samples are thin plates with the  $c$ -axis vertical to the plane. The samples were cleaved and then cut by a wire saw into a rectangular with along the (100) direction in the tetragonal notation. As shown previously,<sup>[5,20]</sup> the resistivity along this direction has minimal effects from nematic fluctuations. The cut samples were glued by GE varnish on the tops of the piezobender and BeCu frame of a home-made uniaxial pressure device,<sup>[5]</sup> as shown in Figs. 1(a) and 1(b). The force applied on the sample was supplied by the piezobender, whose top would try to move under certain voltage. We define the positive values of uniaxial pressure as compressing the sample. We note that the zero pressure is just a nominal value as the voltage applied on the piezobender is zero. The width of the sample was further reduced by an FIB system (Thermo Scientific Helios G4 PFIB CXe DualBeam). The resistance was measured by the four-points method in the physical properties measurement system (Quantum Design, 9 T).

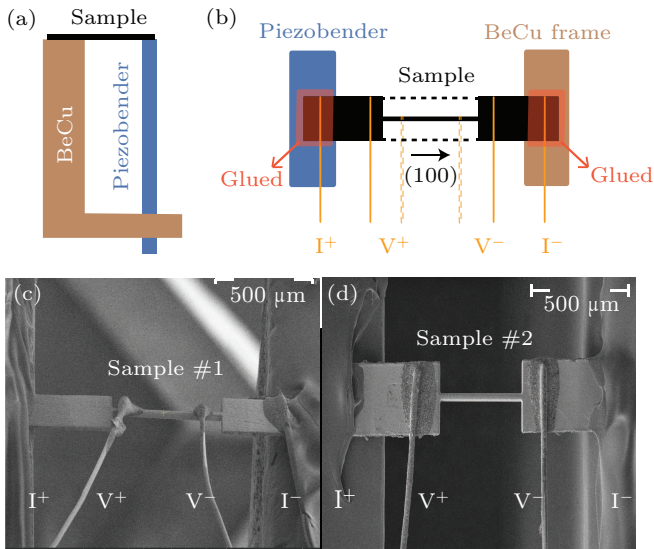


**Fig. 1.** (a) A schematic side view of the home-made uniaxial-pressure device. The bottom of the piezobender is fixed onto the BeCu frame by screws. (b) A schematic top view for the resistance measurements. The dashed lines indicate the edges of the samples before it was cut by the FIB. The force is applied by the piezobender along the (100) direction of the sample. The current electrodes are embedded in the ends of the samples, which are covered with GE varnish. The voltage electrodes are either on the thin bridge or outside the bridge of the sample. (c) and (d) The top-view SEM images of two  $\text{BaFe}_{1.83}\text{Ni}_{0.17}\text{As}_2$  samples, i.e. #1 and #2. The thickness of the sample and width of the bridge in sample #1 are  $45\ \mu\text{m}$  and  $30\ \mu\text{m}$ , respectively. Those in sample #2 are  $30\ \mu\text{m}$  and  $21.4\ \mu\text{m}$ , respectively.

## 3. Results and discussion

Figures 1(c) and 1(d) show the top-view SEM images of two  $\text{BaFe}_{1.83}\text{Ni}_{0.17}\text{As}_2$  samples labeled as #1 and #2. The middle part of both samples is cut by the FIB technique, forming a bridge-like structure. The most important difference between these two samples is that for sample #1, the voltage electrodes are attached on the bridge, while they are outside of the bridge for sample #2, as shown in Fig. 1(b). Apparently, the first setup is better since the voltage electrodes just pick up the voltage drop along the bridge, whereas the voltage signal in the second setup will contain the voltage drops along both the bridge and part of the uncut sample. However, the second setup is easier to success in practice since the bridge in the first setup can be broken when attaching the voltage electrodes.

Figures 2(a) and 2(b) show the uniaxial pressure dependence of the resistance at fixed temperatures for sample #1 above and across the  $T_c$ , respectively. In the normal state, the resistance shows a linear uniaxial pressure dependence up to about  $-0.8$  GPa. With decreasing temperature, nonlinear behaviors appear due to the quick drop of the resistance when the sample becomes superconducting. At low temperatures, the resistance is nonzero at large negative pressure, which means that  $T_c$  is lowered with tensile stress.

The uniaxial pressure dependence of the resistance for sample #2 is shown in Figs. 2(c) and 2(d). The behaviors at positive and negative pressures are very different. Above  $T_c$ , the resistance changes significantly with increasing negative pressure, but the slope becomes much smaller under positive pressure, as shown in Fig. 2(c). The most possible reason of the different slopes is that the directions of the forces from the two ends of the sample are not straightly confined within the sample. Therefore, when the sample is pressed, the sample, especially the bridge, may be bent so that the effective pressure is much smaller than the calculated value. On the other hand, when the sample experiences a tensile strain, it cannot be bent even when the forces are not collinear. During the superconducting transition, a sharp kink feature can be seen and the resistance cannot drop to zero at the positive-pressure region, as shown in Fig. 2(d). These behaviors come from not just the bending of the sample at positive pressure but also the uneven pressure on the bridge and the uncut parts of the sample due to their different cross sections.

To quantitatively study the uniaxial pressure dependence of  $T_c$ , we can pick the resistance values at the same uniaxial pressure and plot them as the function of temperature,<sup>[20]</sup> as shown in Figs. 3(a) and 3(b) for samples #1 and #2, respectively. The drop of  $R-T$  during the superconducting transition in sample #1 is smoothly shifted to lower temperature with increasing negative pressure. For sample #2, there is just one superconducting transition at large negative pressures but a long “tail” exists at positive and small negative pressures. This is

because the voltage electrodes in sample #2 are not directly attached on the bridge so they measure the voltage drop on both the bridge and the uncut parts of the sample. Since the bridge has a much smaller cross section, the pressure applied on it would be much larger than the uncut parts of the sam-

ple. Therefore, when a large negative pressure is applied so that the  $T_c$  of the bridge is much lower than that of the uncut parts, only the superconducting transition in the bridge can be measured since the uncut parts are in the superconducting state and thus its resistance is zero.

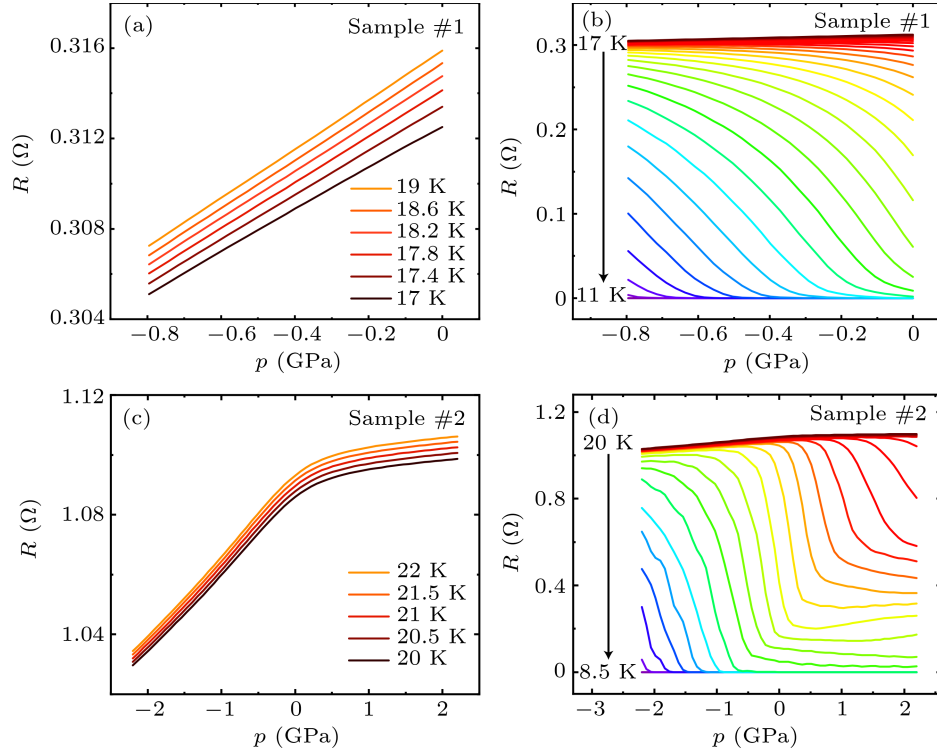


**Fig. 2.** (a) and (c) Uniaxial pressure dependence of the resistance at temperatures just above  $T_c$  for sample #1 and sample #2, respectively. (b) and (d) Uniaxial pressure dependence of the resistance during the superconducting transition for sample #1 and sample #2, respectively.

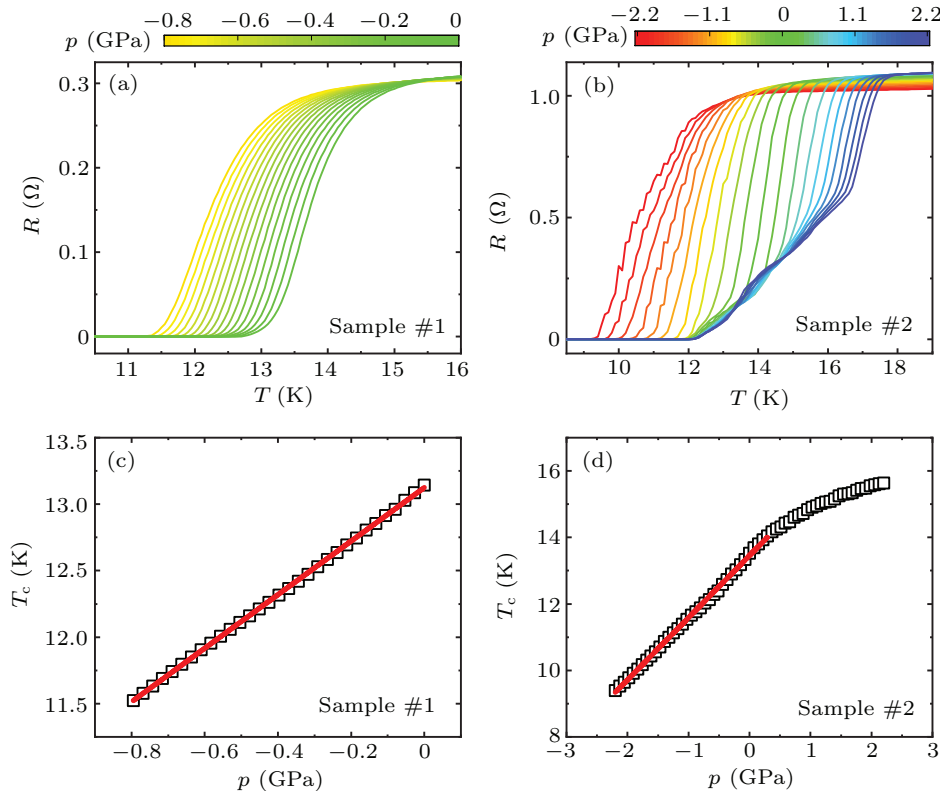


**Fig. 3.** (a) and (b) The temperature dependence of the resistance converted from the uniaxial pressure dependence of the resistance for samples #1 and #2, respectively. (c) and (d) The uniaxial pressure dependence of  $T_c$  for samples #1 and #2. The solid lines are fitted results by a linear function.

On the other hand, when the  $T_c$  of the bridge is higher than that of the uncut parts under a positive pressure, the signal of the voltage electrodes cannot drop to zero after the superconducting transition of the bridge since the uncut parts are still non-superconducting. However, we note that we cannot see two clear superconducting transitions. Rather, a long “tail” exists expanding from about 16.8 K to 12 K, which is probably due to the inhomogeneous pressure around the connections between the bridge and the uncut parts. We also note that the resistance shows discontinuous behavior during the superconducting transition at large negative pressures, probably also coming from the inhomogeneous pressure.

Figures 3(c) and 3(d) show the uniaxial pressure dependence of  $T_c$ , which is obtained by extrapolating the fast drop of the resistance during the superconducting transition to zero resistance. The  $T_c$  of sample #1 shows a linear relationship with the uniaxial pressure, which gives  $dT_c/dp = 2.0$  K/GPa. For sample #2, such linear relationship still holds for negative pressure and gives  $dT_c/dp = 1.9$  K/GPa. At positive pressure, significant deviation appears and the results are not reliable probably due to the bend of the sample.

Our results show that the application of the FIB technique can greatly enhance the uniaxial pressure for our uniaxial pressure device. As shown previously, our device can change the  $T_c$  of  $\text{BaFe}_{2-x}\text{Ni}_x\text{As}_2$  in the order of tens of mK since the maximum force from the piezobender is just about 1 N.<sup>[5,20]</sup> By reducing the width of the sample by the FIB, the uniaxial pressure can be increased by about two orders of magnitude. For the uniaxial pressure device that can apply much larger force,<sup>[19]</sup> this method may also help to increase the maximum strain. As the glue used in such device endures larger shear force, fracture may happen at the interface between the glue and the sample. By cutting the sample with the FIB technique, the large pressure is present at the crossover from the ends of the bridge to the uncut parts of the sample, while the pressure at the interface between the glue and the sample is still small. In our case, the GE varnish, which cannot provide large shear force, can still be used as glue even when the uniaxial pressure on the sample is 2 GPa. Besides the mechanical advantages, the resistance is also significantly increased due to the narrowing of the cross section, which will be very useful to enhance the measurement resolution if a sample’s resistivity is very low.

One of the disadvantages of this method is that the successful probability for the experiment is low since the sample may be broken when the temperature is lowered. The most possible reason for this to happen is because of the thermal expansion from the frame and piezobender. While the actual force applied on the sample may be small, the forces from two ends of the sample may not be strictly along the bridge so that

a sample can be easily broken. In fact, sample #1 was broken when we tried to apply a small positive force. This issue may be improved later by re-designing the frame to use materials with much smaller thermal expansion coefficients. A more accurate way to adjust the alignment between the sample and the frame should also be helpful. Another limit of our method is that only resistivity measurement can be carried out on the bridge, so it cannot be applied for those measurements required a larger volume of the sample, such as heat capacity, elastocaloric effect and nuclear magnetic resonance spectroscopy.<sup>[22–26]</sup>

## 4. Conclusion

We apply the FIB technique to reduce the cross section of the samples in the uniaxial-pressure measurements. The maximum pressure and the resistance can be increased by one to two orders of magnitude, which will enable us to better study the uniaxial pressure dependence of the superconducting transition temperature. Therefore, this method will be useful for further studies of the uniaxial pressure effects on some physical properties for some systems such as superconductors.

## Acknowledgements

Project supported by the National Key Research and Development Program of China (Grant Nos. 2022YFA1403402, 2021YFA1400401, 2020YFA0406003, and 2017YFA0302903), the National Natural Science Foundation of China (Grant Nos. 11961160699 and 11874401), and the Chinese Academy of Sciences (Grant Nos. XDB33000000 and GJTD-2020-01).

## References

- [1] Shapiro M C, Hlobil P, Hristov A T, Maharaj A V and Fisher I R 2015 *Phys. Rev. B* **92** 235147
- [2] Chu J H, Kuo H H, Analytis J G and Fisher I R 2012 *Science* **337** 6095
- [3] Riggs S C, Shapiro M, Maharaj A V, Raghu S, Bauer E, Baumbach R, Giraldo-Gallo P, Wartenbe M and Fisher I 2015 *Nat. Commun.* **6** 6425
- [4] Kuo H H, Chu J H, Palmstrom J C, Kivelson S A and Fisher I R 2016 *Science* **352** 958
- [5] Liu Z, Gu Y, Zhang W, Gong D, Zhang W, Xie T, Lu X, Ma X, Zhang X, Zhang R, Zhu J, Ren C, Shan L, Qiu X, Dai P, Yang Y F, Luo H and Li S 2016 *Phys. Rev. Lett.* **117** 157002
- [6] Gu Y, Liu Z, Xie T, Zhang W, Gong D, Hu D, Ma X, Li C, Zhao L, Lin L, Xu Z, Tan G, Chen G, Meng Z Y, Yang Y F, Luo H and Li S 2017 *Phys. Rev. Lett.* **119** 157001
- [7] Ishida K, Tsujii M, Hosoi S, Mizukami Y, Ishida S, Iyo A, Eisaki H, Wolf T, Grube K, Löhneysen H, Fernandes R M and Shibauchi T 2020 *Proc. Natl. Acad. Sci. USA* **117** 6424
- [8] Ishida K, Hosoi S, Teramoto Y, Usui T, Mizukami Y, Itaka K, Matsuda Y, Watanabe T and Shibauchi T 2020 *J. Phys. Soc. Jpn.* **89** 064707
- [9] Bartlett J M, Steppke A, Hosoi S, Noad H, Park J, Timm C, Shibauchi T, Mackenzie A P and Hicks C W 2021 *Phys. Rev. X* **11** 021038
- [10] Wiecki P, Frachet M, Haghighirad A A, Wolf T, Meingast C, Heid R and Böhmner A E 2021 *Nat. Commun.* **12** 4824
- [11] Xie T, Liu Z, Gu Y, Gong D, Mao H, Liu J, Hu C, Ma X, Yao Y, Zhao L, Zhou X, Schneeloch J, Gu G, Danilkin S, feng Yang Y, Luo H and Li S 2022 *J. Phys.: Condens. Matter* **34** 334001

- [12] Wang X, Gong D, Liu B, Ma X, Zhao J, Wang P, Sheng Y, Guo J, Sun L, Zhang W, Lai X, Tan S, Feng Y, and Li S **2022 *Chin. Phys. Lett.* **39** 107101**
- [13] Mao H C, Gong D L, Ma X Y, Luo H Q, Yang Y F, Shan L and Li S L **2018 *Chin. Phys. B* **27** 087402**
- [14] Hicks C W, Brodsky D O, Yelland E A, Gibbs A S, Bruin J A N, Barber M E, Edkins S D, Nishimura K, Yonezawa S, Maeno Y and Mackenzie A P **2014 *Science* **344** 6181**
- [15] Steppke A, Zhao L, Barber M E, Scaffidi T, Jerzembeck F, Rosner H, Gibbs A S, Maeno Y, Simon S H, Mackenzie A P and Hicks C W **2017 *Science* **355** 6321**
- [16] Stern A, Dzero M, Galitski V M, Fisk Z and Xia J **2017 *Nat. Mater.* **16** 708**
- [17] Kim H H, Souliou S M, Barber M E, Lefrancois E, Minola M, Tortora M, Heid R, Nandi N, Borzi R A, Garbarino G, Bosak A, Porras J, Loew T, König M, Moll P J W, Mackenzie A P, Keimer B, Hicks C W and Tacon M L **2018 *Science* **362** 1040**
- [18] Malinowski P, Jiang Q, Sanchez J J, Mutch J, Liu Z, Went P, Liu J, Ryan P J, Kim J W and Chu J H **2020 *Nat. Phys.* **16** 1189**
- [19] Hicks C W, Barber M E, Edkins S D, Brodsky D O and Mackenzie A P **2014 *Rev. Sci. Instrum.* **85** 065003**
- [20] Liu Z, Gu Y, Hong W, Xie T, Gong D, Ma X, Liu J, Hu C, Zhao L, Zhou X, Fernandes R M, Yang Y F, Luo H and Li S **2019 *Phys. Rev. Research* **1** 033154**
- [21] Chen Y, Lu X, Wang M, Luo H and Li S **2011 *Supercond. Sci. Technol.* **24** 065004**
- [22] Li Y S, Borth R, Hicks C W, Mackenzie A P and Nicklas M **2020 *Rev. Sci. Instrum.* **91** 103903**
- [23] Ikeda M S, Straquadine J A W, Hristov A T, Worasaran T, Palmstrom J C, Sorensen M, Walmsley P and Fisher I R **2019 *Rev. Sci. Instrum.* **90** 083902**
- [24] Straquadine J A W, Ikeda M S and Fisher I R **2022 *Phys. Rev. X* **12** 021046**
- [25] Kissikov T, Sarkar R, Lawson M, Bush B T, Timmons E I, Tanatar M A, Prozorov R, Bud'ko S L, Canfield P C, Fernandes R M and Curro N J **2018 *Nat. Commun.* **9** 1058**
- [26] Luo Y, Pustogov A, Guzman P, Dioguardi A P, Thomas S M, Ronning F, Kikugawa N, Sokolov D A, Jerzembeck F, Mackenzie A P, Hicks C W, Bauer E D, Mazin I I and Brown S E **2019 *Phys. Rev. X* **9** 021044**